Characteristics of Crack Interior Initiation and Early Growth Originated from Inclusion for Very-High-Cycle Fatigue of High Strength Steels

Youshi Hong*, Zhengqiang Lei, Chengqi Sun and Aiguo Zhao

LNM, Institute of Mechanics, Chinese Academy of Sciences, Beijing 100190, China
*Corresponding author, email: hongys@imech.ac.cn

ABSTRACT. *Fatigue tests on a high carbon chromium steel were performed with rotating bending and ultrasonic fatigue tests. The fractography was examined to reveal that fatigue cracks initiated at specimen interior for very-high-cycle fatigue (VHCF) with fish-eye pattern embracing fine-granular-area (FGA) morphology originated from inclusions. The measurements show the dimensions of FGA and fish-eye as a function of the applied stress and fatigue failure cycles. The results also show the values of stress intensity factor range at FGA (ΔK_{FGA}) and fish-eye ($\Delta K_{fisheye}$) almost keep constant with failure cycles, and the values of ΔK_{FGA} are close to the relevant fatigue threshold (ΔK_{th}). The fatigue life from FGA to fish-eye and from fish-eye to the critical crack size is respectively calculated, thus to estimate the fatigue life contributed by FGA. Moreover, the crack growth rate within FGA was estimated. The present result is combined with our previous ones and with those available in literature to discuss the process of crack initiation and early growth for VHCF, which is responsible for a majority part of total fatigue life. In addition, the large scattering of fatigue life was investigated, which was ascribed to the distribution of inclusion size.*

INTRODUCTION

In very-high-cycle fatigue (VHCF) regime for high strength steels, the period of crack initiation and early growth almost dominates the fatigue life [1,2]. The process of the crack initiation at VHCF regime is prone to originate at the inclusion from the interior of specimen with the pattern of fish-eye embracing FGA (fine-granular-area) or called ODA (optical-dark-area) [3,4].

In this paper, fatigue tests on a high carbon chromium steel were performed with rotating bending and ultrasonic fatigue testing methods. The fractography of broken specimens was examined via scanning electron microscopy. The values of stress intensity factor range at FGA and fish-eye were calculated, and the crack growth rate within FGA was estimated. The present result is combined with our previous ones [5-9] and with those available in literature [10-13] to explain the crack growth process in the early stage of VHCF, which is responsible for a majority part of total fatigue life. In addition, the large scattering of fatigue life was also investigated.

EXPERIMENTAL PROCEDURE

The test material of this investigation is a high carbon chromium steel with the main chemical compositions of 1.06 %C and 1.04 %Cr (Fe balance). Two types of hourglass shape specimens were machined from the annealed material bar. The dimensions of the specimens are shown in Fig. 1. Such specimens were heat-treated: austenitized at 845 °C for 2 hours in vacuum, then oil-quenched and tempered for 2.5 hours in vacuum at 150 °C and 180 °C, respectively. The two groups of specimens are named TT150 and TT180, respectively. The surface of the diameter reduced part for each specimen was ground and polished to a smooth finish thus to eliminate the machining scratches. The average ultimate tensile strength is 2163 MPa for TT150 and 1849 MPa for TT180, respectively, which were obtained from the tensile tests on 4 specimens (ϕ5 mm) per group with the same heat-treatment procedure.

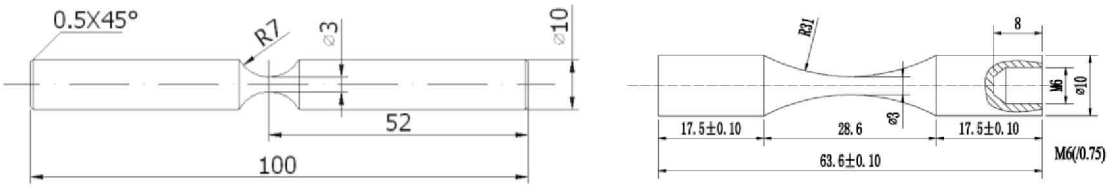

a **b**

Figure 1. Shapes and dimensions of two types of specimens for fatigue tests, (a) for rotating bending test, and (b) for ultrasonic fatigue test.

Fatigue tests were performed in two loading schemes, namely rotating bending (RB) and ultrasonic fatigue (UL), respectively.

The RB tests were performed by using a "Giga-Quad" machine at room temperature with the rotating speed of 3150 rpm *i.e.* the frequency of 52.5 Hz and the stress ratio of −1. The machine is capable for four specimens tested simultaneously. A weight was placed to the end of specimen through a fixture as a cantilever type loading. TT180 specimens were tested by using RB method and the range of the applied maximum stress (σ_{max}) was ranging from 730 MPa to 1150 MPa, so as to gain the whole spectrum of S-N data of the test material.

The UL testing was conducted by using a Shimadzu USF-2000 at a resonance frequency of 20 kHz at room temperature, with a resonance interval of 100 ms per 500 ms and the stress ratio of −1. Compressive air was used to cool specimen surface during UL testing. TT150 specimens were tested by using UL method. The applied maximum stress was within a small range between 860 MPa and 880 MPa. This was aimed to examine the scattering characteristics of fatigue strength for the test material.

The fracture surfaces of failure specimens were examined by using a field-emission type of scanning electron microscope (SEM). The local area of crack initiation region was carefully examined. The characteristic dimensions for crack initiation region, *i.e.* the sizes of FGA and fish-eye, were measured from SEM photos.

EXPERIMENTAL RESULTS

The photos shown in Fig. 2 are an example of the typical morphology of interior crack initiation for VHCF regime of TT180 specimens subjected to RB loading, for which the dimensions are: $2a_{inc}$=35.3μm, $2a_{FGA}$=66.3μm, and $2a_{fisheye}$=206.2μm. Since RB loading leads to the largest stress at specimen surface, the crack initiation of fish-eye almost formed underneath the surface and grew towards the surface then transformed into the next stage of crack growth. For UL fatigue of axial loading, the sites for interior crack initiation were almost randomly distributed in the cross-section.

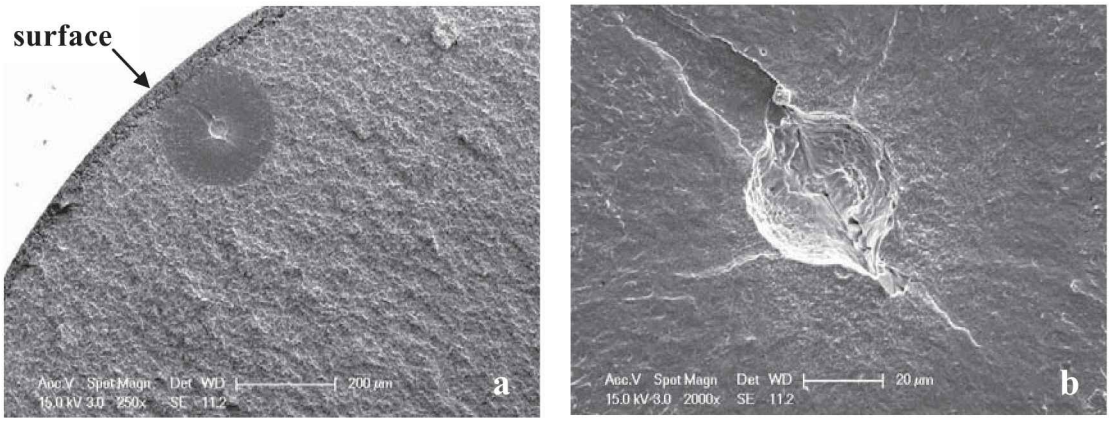

Figure 2. SEM photos showing fractography of a TT180 specimen (RB-4), σ_{max}=808 MPa, N_f=1.79×10^7; (a) crack initiation region with whole fish-eye morphology, and (b) enlargement showing FGA surrounding the crack origin.

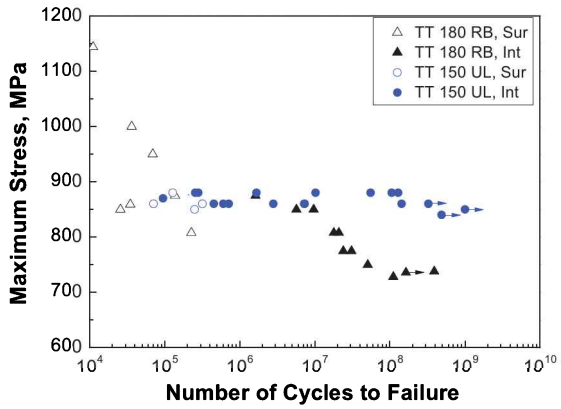

Figure 3. Fatigue test results for two groups of specimens.

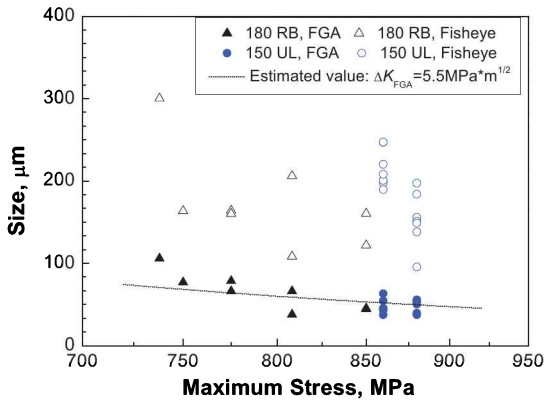

Figure 4. FGA and fish-eye sizes versus applied maximum stress.

Table 1 lists the measurement data of the characteristic dimensions for crack initiation of the two groups of specimens together with the values of the applied

maximum stress and the fatigue life. Figure 3 shows the results of S-N relation for the two groups of specimens, in which the datum points also symbolize the crack initiation mode at surface or from interior of specimen. It is seen from Table 1 and Fig. 3 that, for TT180 specimens subjected to RB cycling, the fatigue life (N_f) is from 10^4 to 4×10^8; the S-N data present a duplex or step-wise tendency. For TT150 specimens subjected to UL cycling at almost the same level of the maximum stress (860~880 MPa), the results show a very large scattering of data distribution. The difference of the fatigue life is as large as three orders of magnitude, ranging from 10^5 to 10^8.

Figure 4 shows the measurements of both FGA and fish-eye sizes as a function of the applied maximum stress. It is seen from Table 1 and Fig. 4 that the FGA sizes are within a relatively small range between 40 and 100 μm and the fish-eye sizes are distributed in a large range between 100 and 300 μm.

Table 1. Measurement results of crack initiation parameters for two groups of specimens with the data of applied maximum stress and fatigue life

Specimen code	σ_{max} (MPa)	N_f	$2a_{Inc}$ (μm)	$2a_{FGA}$ (μm)	$2a_{fisheye}$ (μm)
RB-1	850	5.60×10^6	38.1	45.5	160.5
RB-2	850	9.64×10^6	28.2	44.4	121.9
RB-3	808	2.09×10^7	30.1	37.8	108.3
RB-4	808	1.79×10^7	35.3	66.3	206.2
RB-5	775	2.40×10^7	46.8	78.8	160.2
RB-6	775	3.08×10^7	39.5	66.3	164.2
RB-7	750	5.08×10^7	39.9	76.9	163.6
RB-8	738	3.89×10^8	42.3	106.0	300.3
UL-1	860	4.53×10^5	41.1	43.3	208.1
UL-2	860	7.15×10^5	40.1	45.4	189.6
UL-3	860	6.06×10^5	59.5	63.2	200.8
UL-4	880	7.05×10^5	52.1	54.1	183.9
UL-5	880	1.67×10^6	48.9	55.8	138.1
UL-6	860	2.81×10^6	37.5	44.5	220.4
UL-7	860	7.20×10^6	36.7	43.7	247.1
UL-8	860	7.33×10^6	32.5	54.4	197.6
UL-9	880	1.09×10^7	29.5	37.6	197.4
UL-10	880	1.02×10^7	29.2	50.4	155.9
UL-11	880	5.54×10^7	19.9	39.6	95.5
UL-12	860	1.43×10^8	19.5	37.5	247.0
UL-13	880	1.29×10^8	30.8	52.8	151.3

The range of stress intensity factor at the periphery of inclusion (ΔK_{Inc}), FGA (ΔK_{FGA}) and fish-eye ($\Delta K_{fisheye}$) is calculated by using the following equation [14]:

$$\Delta K = 0.5\Delta\sigma_a\sqrt{\pi\sqrt{area}} \quad (1)$$

where $\Delta\sigma_a$ is applied stress amplitude and $\sqrt{area}$ is the equivalent size of inclusion, FGA or fish-eye. The values of ΔK_{FGA} are almost between 5 and 6 MPa·m$^{1/2}$, the values of ΔK_{Inc} are below ΔK_{FGA} with a slight decrease trend with failure cycles and the values of $\Delta K_{fisheye}$ almost keep constant around 10 MPa·m$^{1/2}$.

DISCUSSION

The present results show that the sizes of FGA distributed within a given range and the values of ΔK_{FGA} converged almost between 5 and 6 MPa·m$^{1/2}$. This supports our previous result that the values of ΔK_{FGA} keep constant with the average value close to the crack growth threshold (ΔK_{th}) [8].

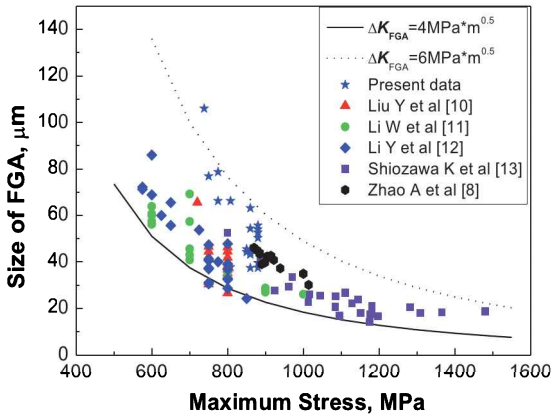

Figure 5. FGA size versus σ_{max}.

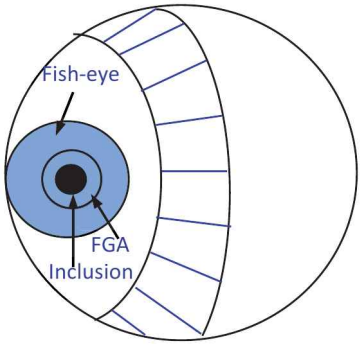

Figure 6. Schematic of fracture surface.

Here, we collect more data from our previous results [8] and others from literature [10-13] in addition to our present ones to demonstrate the relationship between ΔK and σ_{max} as shown in Fig.5. Note that the relation between ΔK and σ_{max} is governed by Eq. 1 and the two curves as the lower bound (ΔK_{FGA}=4 MPa·m$^{1/2}$) and the upper bound (ΔK_{FGA}=6 MPa·m$^{1/2}$) embracing almost all the data. The present investigation confirms that the equivalent diameter of FGA is the intrinsic chacracteristic size of crack initiation for the fatigue crack originating from the interior of specimen. It is proposed that for crack interior initiation mode, there exists an intrinsic characteristic size related to ΔK_{th}. In some cases, the pattern of this size is clearly observed like FGA. However in some other cases, although the pattern of this size is not clear, the size intrinsically exists. Based on this, one is able to estimate the fatigue life contributed before and after crack initiation, and to estimate the crack extension rate in the crack initiation stage within FGA.

Figure 6 is a schematic drawing to illustrate the general frame of fatigue crack origination from the interior of specimen as shown in Fig. 2. As revealed by the present result and together with previous ones, the value of ΔK_{FGA} corresponds to that of ΔK_{th}. It

is assumed that Paris relation is acceptable to describe the crack growth process after ΔK_{th}, *i.e.* ΔK_{FGA}. Therefore, Paris equation is used to calculate the fatigue life (N_1) from the boundary of FGA to that of fish-eye and the fatigue life (N_2) from fish-eye to the critical boundary given by the fracture toughness of the material. The equations are:

$$\frac{da}{dN} = A\Delta K^m \tag{2}$$

$$N_1 = \frac{2}{(m-2)AY^m\Delta\sigma^m}\left[\frac{1}{a_{FGA}^{(m-2)/2}} - \frac{1}{a_{fisheye}^{(m-2)/2}}\right] \tag{3}$$

where A and m are the parameters in relation with the given material. For the material tested in this investigation, we noticed a similar case with the crack growth data [15] and obtained the values of A=1.03×10^{-12} and m=3.28 with respect to the dimensions of da/dN (m/cycle) and ΔK (MPa·m$^{1/2}$), which was then used in the fatigue life estimation.

The results of N_1 and N_2 for each specimen of the two groups are listed in Table 2. The fatigue life contributed by crack initiation (N_i) is $N_i = N_f - N_1 - N_2$. The values of N_i/N_f for each specimen of the two groups are obtained and also listed in Table 2, which are plotted in Fig. 7. A group of our previous data [8] are also added to Fig. 7. For explicitness, the data of N_f are again listed in Table 2.

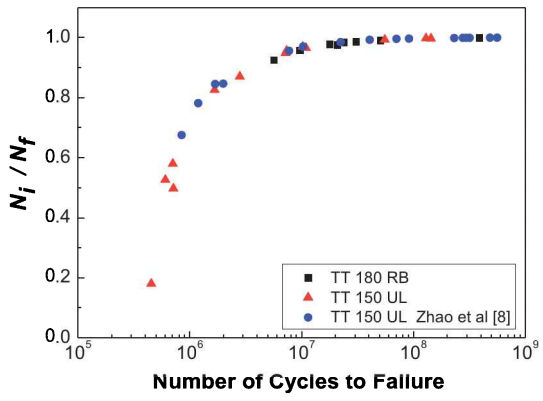

Figure 7. Normalized crack initiation life Versus total fatigue life.

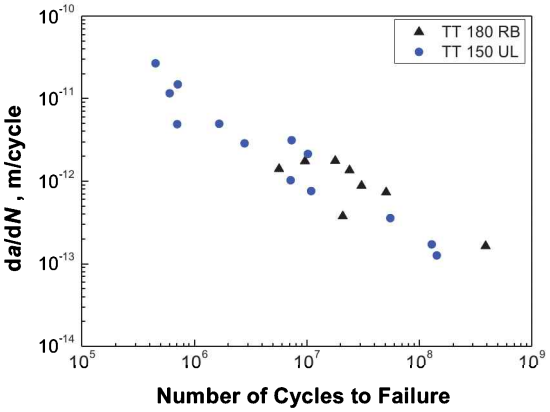

Figure 8. Crack extension rate within FGA as a function of fatigue life.

From Fig. 7 and Table 2, it is seen that the value of N_i/N_f increases dramatically with total fatigue life (N_f). The crack initiation life (N_i) due to FGA is less than 70% when the total fatigue life is below 10^6 cycles. For total fatigue life is between 10^6 and 10^7 cycles, the ratio of N_i/N_f increases to 70% and 95%, and for the total fatigue life is beyond 10^7 cycles, *i.e.* the VHCF regime, the value of N_i/N_f is larger than 95%. Especially for the total fatigue life is above 5×10^7 cycles, the value of N_i/N_f is larger

than 99%. It is evident that for fatigue damage including VHCF regime, the fatigue life is almost consumed by crack initiation process, *i.e.* the formation of FGA.

Table 2. Calculation results of N_1, N_2, N_i and da/dN within FGA for two groups of specimens

Specimen code	N_f	N_2 (N_2/N_f) $a_{fisheye}$ to a_{K1c}	N_1 (N_1/N_f) a_{FGA} to $a_{fisheye}$	N_i/N_f $a<a_{FGA}$	da/dN (m/cycle) $a<a_{FGA}$
RB-1	5.60×10^6	5.78×10^4(1.02%)	3.71×10^5(6.54%)	92.5%	1.41×10^{-12}
RB-2	9.64×10^6	7.18×10^4(0.75%)	3.39×10^5(3.51%)	95.7%	1.75×10^{-12}
RB-3	2.09×10^7	9.28×10^4(0.44%)	4.28×10^5(2.04%)	97.5%	3.75×10^{-13}
RB-4	1.79×10^7	5.55×10^4(0.31%)	3.51×10^5(1.96%)	97.7%	1.77×10^{-12}
RB-5	2.40×10^7	7.83×10^4(0.33%)	3.22×10^5(1.34%)	98.3%	1.35×10^{-12}
RB-6	3.08×10^7	7.68×10^4(0.25%)	3.72×10^5(1.21%)	98.5%	8.83×10^{-13}
RB-7	5.08×10^7	8.57×10^4(0.17%)	3.87×10^5(0.76%)	99.1%	7.35×10^{-13}
RB-8	3.89×10^8	5.37×10^4(0.01%)	3.69×10^5(0.09%)	99.9%	1.64×10^{-13}
UL-1	4.53×10^5	4.49×10^4(9.91%)	3.26×10^5(72.04%)	18.1%	2.67×10^{-11}
UL-2	7.15×10^5	4.85×10^4(6.79%)	3.10×10^5(43.45%)	49.8%	1.48×10^{-11}
UL-3	6.06×10^5	4.62×10^4(7.64%)	2.41×10^5(39.75%)	52.6%	1.16×10^{-11}
UL-4	7.05×10^5	4.61×10^4(6.54%)	2.50×10^5(35.44%)	58.0%	4.89×10^{-12}
UL-5	1.67×10^6	5.81×10^4(3.49%)	2.32×10^5(13.91%)	82.6%	4.95×10^{-12}
UL-6	2.81×10^6	4.27×10^4(1.52%)	3.21×10^5(11.46%)	87.0%	2.87×10^{-12}
UL-7	7.20×10^6	3.87×10^4(5.38%)	3.30×10^5(4.58%)	94.9%	1.02×10^{-12}
UL-8	7.33×10^6	4.69×10^4(0.64%)	2.71×10^5(3.70%)	95.7%	3.13×10^{-12}
UL-9	1.09×10^7	4.35×10^4(0.39%)	3.35×10^5(3.06%)	96.5%	7.59×10^{-13}
UL-10	1.02×10^7	5.28×10^4(0.52%)	2.58×10^5(2.52%)	97.0%	2.13×10^{-12}
UL-11	5.54×10^7	7.72×10^4(0.14%)	2.88×10^5(0.52%)	99.3%	3.57×10^{-13}
UL-12	1.43×10^8	3.87×10^4(0.03%)	3.70×10^5(0.26%)	99.7%	1.26×10^{-13}
UL-13	1.29×10^8	5.41×10^4(0.04%)	2.47×10^5(0.19%)	99.8%	1.71×10^{-13}

From Fig. 8 and Table 2, it is seen that the value of crack extension rate within FGA, $da/dN\big|_{FGA}$, is between 10^{-11} and 10^{-13} m/cycle, and the value decreases with fatigue life, N_f. For N_f between 10^6 and 10^7, the values of $da/dN\big|_{FGA}$ are within the range of 10^{-11} and 10^{-12} m/cycle. For N_f between10^7 and 4×10^8, *i.e.* VHCF regime, the values of $da/dN\big|_{FGA}$ are in the range from 10^{-12} to 10^{-13} m/cycle.

The data shown in Fig. 2 and Table 1 illustrate a large scattering of fatigue life at the same stress level for TT150 specimens. The observations and measurements on the inclusions from which the cracks originate show that the range of inclusion size, $2a_{Inc}$, is between 20 and 60 μm (Table 1), and the value is inversely proportional to the fatigue life. For N_f between 10^6 and 10^7, the value of $2a_{Inc}$ is ranging from 30 to 50μm. For N_f between10^7 and 4×10^8, *i.e.* VHCF regime, the value of $2a_{Inc}$ is ranging from 20 to 30 μm, substantially smaller than the size before VHCF regime. It is evident that the inclusion size is responsible for the large scattering of fatigue life, which is the weakest link phenomenon.

CONCLUSIONS

1. For crack interior initiation for VHCF, there exists a characteristic dimension, *i.e.* the diameter of FGA, which corresponds to the threshold size of crack propagation.
2. The value of ΔK_{FGA} is a constant and corresponds to ΔK_{th} for a given material. The value is between 4 and 6 MPa·m$^{1/2}$ for the high strength steels.
3. The crack initiation life due to FGA is larger than 95% for the fatigue damage including VHCF regime and is larger than 99% for N_f beyond 5×10^7 cycles.
4. $da/dN\big|_{FGA}$ ranges from 10^{-11} to 10^{-12} m/cycle for N_f between 10^6 and 10^7, and ranges from 10^{-12} to 10^{-13} m/cycle for N_f between 10^7 and 4×10^8, *i.e.* VHCF regime.
5. Large scattering of N_f is related to the large range of inclusion size distribution.

ACKNOWLEDGEMENTS

This investigation was supported by the National Natural Science Foundation of China (Nos. 11172304 and 11021262).

REFERENCES

1. Wang, Q.Y., Berard, J.Y., Dubarre, A., Baudry, G., Rathery, S. and Bathias, C. (1999) *Fatigue Fract. Eng. Mater. Struct.* **22**, 667-672.
2. Marines-Garcia, I., Paris, P.C., Tada, H. and Bathias, C. (2007) *Mater. Sci. Eng. A* **468-470**, 120-128.
3. Hong, Y., Zhao, A. and Qian, G. (2009) *Acta Metall. Sinica* **45**, 769-80.
4. Duan, Z., Shi, H. and Ma, X. (2011) *Fatigue Fract. Eng. Mater. Struct.* **34**, 832-837.
5. Zhou, C., Qian, G. and Hong, Y. (2006) *Key Eng Mater.* **324-325**, 1113-1116.
6. Hong, Y., Zhao, A., Qian, G. and Zhou, C. (2012) *Metall. Mater. Trans. A*, DOI: 10.1007/s11661-011-0816-7.
7. Sun, C., Xie, J., Zhao, A., Lei, Z. and Hong, Y. (2012) *Fatigue Fract. Eng. Mater. Struct.* **35**, DOI: 10.1111/j.1460-2695.2011.01658.x
8. Zhao, A., Xie, J., Sun, C., Lei, Z. and Hong, Y. (2011) *Mater. Sci. Eng. A* 528, 5872-5877.
9. Zhao, A., Xie, J., Sun, C., Lei, Z. and Hong, Y. (2012) *Int. J. Fatigue* **38,** 46-56.
10. Liu, Y.B., Li, Y.D., Li, S.X., Yang, Z.G., Chen, S.M., Hui, W.J. and Weng, Y.Q. (2010) *Int. J. Fatigue* **32**, 1351-1357.
11. Li, W., Sakai, T., Li, Q., Lu, L.T. and Wang, P. (2010) *Int. J. Fatigue* **32**, 1096-1107.
12. Li, Y.D., Yang, Z.G., Li, S.X., Liu, Y.B. and Chen, S.M. (2008) *Acta Metall. Sinica* **44**, 968-972.
13. Shiozawa, K., Morii, Y., Nishino, S. and Lu, L. (2006) *Int. J. Fatigue* **28**, 1521-1532.
14. Murakami, Y., Kodama, S. and Konuma, S. (1988) *Trans. JSME* **54A**, 688-695.
15. Shiozawa, K., Lu, L. and Ishihara, S. (2001) *Fatigue Fract. Eng. Mater. Struct.* **24**, 781-790.